

## HUBBLE SPACE TELESCOPE OBSERVATIONS OF THE OPTICAL JETS OF PKS 0521–365, 3C 371, AND PKS 2201+044

RICCARDO SCARPA

Space Telescope Science Institute, 3700 San Martin Drive, Baltimore, MD 21218; scarpa@stsci.edu

C. MEGAN URRY

Space Telescope Science Institute, 3700 San Martin Drive, Baltimore, MD 21218; cmu@stsci.edu

RENATO FALOMO

Osservatorio Astronomico di Padova, Vicolo dell'Osservatorio 5, 35122 Padova, Italy; falomo@astrpd.pd.astro.it

AND

ALDO TREVES

University of Insubria Como; University of Milan at Como, Via Lucini 3, Como, Italy; treves@uni.mi.astro.it

Received 1999 May 3; accepted 1999 July 15

### ABSTRACT

*Hubble Space Telescope (HST)* observations have led to the discovery of the optical counterpart of the radio jet of PKS 2201+044 and to a detailed analysis of the optical jets of PKS 0521–365 and 3C 371. At *HST* spatial resolution these jets are well resolved, displaying knotty morphologies. When compared with radio maps of appropriate resolution, a clear one-to-one correspondence between optical and radio structures is found, showing that all detected optical structures are indeed related to the radio synchrotron emission. Photometry of the brightest knots shows that the radio-to-optical spectral index and the derived intensity of the equipartition magnetic field are approximately constant along the jet. Thus, present observations suggest that the electron energy distribution does not change significantly all along the jet.

*Subject headings:* BL Lacertae objects: individual (3C 371, PKS 0521–365, PKS 2201+044) — galaxies: jets

### 1. INTRODUCTION

Radio-emitting synchrotron jets are commonly observed in radio galaxies and quasars. In contrast, the optical counterparts of these structures are observed only rarely (e.g., O’Dea et al. 1999; Scarpa & Urry 1999 and references therein). The high spatial resolution of the *Hubble Space Telescope (HST)* allows the study of known optical jets with detail comparable to VLA radio maps and has led to the discovery of new optical jets. *HST* is particularly useful for finding short jets that develop within few arcseconds from the luminous nucleus and/or are fully contained within a luminous host galaxy. The jet emission is typically confined to a narrow area, so at higher spatial resolution its surface brightness is higher. This facilitates detection closer to the nucleus, increasing the probability of detecting either shorter jets or jets more closely aligned with the line of sight. Not surprisingly, the number of known jets has almost doubled since the introduction of *HST* (e.g., Sparks et al. 1995; Ridgway & Stockton 1997).

Detection of optical emission and high-resolution optical imaging of radio jets put important constraints on jet physics. For example, electrons radiating at  $\nu \sim 10^{15}$  Hz in a typical equipartition magnetic field of  $10^{-4}$  G have a radiative cooling time of only  $t_{1/2} \sim 1000$  years, yet optical jets are tens of thousands of light-years long (e.g., PKS 0521–365; Danziger et al. 1979).

Here we present new *HST* images<sup>1</sup> of three relativistic jets which probe the shortest lived radiating particles. The

observations were obtained as part of our *HST* snapshot survey of BL Lac objects (Urry et al. 1999; Scarpa et al. 1999) and so were shorter than the ideal for studying synchrotron jets; however, the large number of low-redshift BL Lac observed greatly increased our chance of detecting new jets. Indeed, in PKS 2201+044, the 104th of 109 objects observed, we discovered a new optical jet. We also imaged two well-known BL Lacertae objects with previously known optical jets, PKS 0521–365 and 3C 371, which are relatively nearby and can be studied in great detail with *HST*.

Throughout the paper  $H_0 = 50 \text{ km s}^{-1} \text{ Mpc}^{-1}$  and  $q_0 = 0$  were used.

### 2. OBSERVATIONS AND DATA ANALYSIS

Observations were carried out with the *Hubble Space Telescope* in snapshot mode, using the Wide Field and Planetary Camera 2 (WFPC2) through filters F702W (for PKS 0521–365 and PKS 2201+044) and F555W (for 3C 371). Targets were centered on the PC chip, which has pixels  $0''.046$  wide. To obtain a final image well exposed both in the inner, bright nucleus and in the outer, fainter regions, we set up a series of exposures with duration ranging from a few to hundreds of seconds, for total integration times of 305, 302, and 610 s for PKS 0521–365, 3C 371, and PKS 2201+044, respectively.

After standard reduction (flat-field, dark and bias subtraction, and flux calibration carried out as part of the standard *HST* pipeline processing), images were combined using the task CRREJ available within IRAF. This task stacks all images while removing cosmic-ray events. Final images were flux-calibrated following the prescription of Holtzman et al. (1995, their eq. [9] and Table 10).

<sup>1</sup> Based on observations made with the NASA/ESA *Hubble Space Telescope*, obtained at the Space Telescope Science Institute, which is operated by the Association of Universities for Research in Astronomy, Inc., under NASA contract NAS 5-26555.

Although readily visible in the direct *HST* image, to be fully studied the jet must be separated from the contaminating light of the host galaxy and the central, luminous point source. We therefore first subtracted a suitably scaled point-spread function (PSF) model computed using Tiny Tim software (Krist 1995), plus an estimate of large-angle scattered light (Scarpa et al. 1999). With the IRAF task ELLIPSE we then fitted the residual light with a two-dimensional elliptical galaxy model, convolved with the PSF. Extraneous features, including the jet itself, were masked before fitting the isophotes. (For details on host galaxies see Scarpa et al. 1999 and Falomo et al. 1999.) The final jet image was obtained after subtracting both PSF and galaxy models.

### 3. DESCRIPTION OF THE THREE JETS

#### 3.1. PKS 0521–365

This well-studied nearby object ( $z = 0.0554$ ; Danziger et al. 1979) is one of the most remarkable extragalactic objects known, as it shows a variety of nuclear and extranuclear phenomena. First classified as an N galaxy, then as a BL Lac, now it shows the strong narrow and broad emission lines typical of Seyfert 1 galaxies (Ulrich 1981; Scarpa, Falomo, & Pian 1995). Most interesting, the source has a prominent radio and optical jet (Danziger et al. 1979; Keel 1986; Macchetto et al. 1991; Falomo 1994), which resembles that of the nearby radio galaxy M87 (Sparks, Biretta, & Macchetto 1994).

The optical jet as observed at *HST* resolution (Fig. 1) has a structure characterized by a bright feature near the nucleus (marked with an F), which is, however, too close to the bright central point source to be readily studied. It cor-

responds to the base of the jet visible in the UV image obtained with the *HST* Faint Object Camera (Macchetto et al. 1991). Farther out, a prominent bright spot (called A following Falomo 1994), a series of smaller knots and a final bright spot (C) are also visible. Structure B is resolved into at least three distinct knots aligned along the jet axis. Structure C (also called the “red tip”) is  $9''.2$  from the nucleus and has integrated magnitude  $m_R = 21.3 \pm 0.2$  mag. It is clearly resolved even if its symmetric shape makes it appear point-like, and its radial profile is consistent with an elliptical galaxy. This confirms the finding of Falomo (1994) and, together with the absence of radio emission (Keel 1986) and detectable optical polarization (Sparks, Miley, & Macchetto 1990), suggests that the “red tip” is a background galaxy (or small companion) rather than part of the jet, in spite of the almost perfect alignment.

Finally, we note that in the optical there is no indication of either a counterjet or the 2 cm bright hot spot reported by Keel (1986) southeast of the nucleus, which was also not detected in deeper ground-based observations (Falomo 1994).

We were able to measure the apparent magnitude of five bright knots. In Table 1 we report the apparent *R* magnitude, the distance of each feature from the central point source, and the jet width at these positions. The reported jet width is the average full width at zero intensity estimated averaging on strips 10 pixels wide. Errors on the jet width are  $\pm 0''.2$  for all values. The total magnitude of the jet, excluding knots C and F, is  $m_R = 19.9 \pm 0.2$  mag.

The jet is resolved also orthogonal to the axis. In feature D two knots are clearly visible, E is tilted with respect to the jet axis, and around B several secondary maxima of light are detected. Indeed, compared with lower resolution

TABLE 1  
PHYSICAL PROPERTIES OF THE JETS<sup>a</sup>

| Structure       | Band     | $m_R$          | Distance <sup>b</sup> | Width <sup>c</sup> | $F_R$ <sup>d</sup> | $\alpha_{RO}$    | Size <sup>e</sup> | $B^f$         |
|-----------------|----------|----------------|-----------------------|--------------------|--------------------|------------------|-------------------|---------------|
| PKS 0521–365    |          |                |                       |                    |                    |                  |                   |               |
| Jet total ..... | <i>R</i> | $19.2 \pm 0.2$ | ...                   | ...                | 106                | $-0.73 \pm 0.05$ | 28.6              | $5.6 \pm 0.7$ |
| Jet – A .....   |          | $19.9 \pm 0.3$ | ...                   | ...                | 46                 | $-0.67 \pm 0.06$ | 22.8              | $4.6 \pm 0.6$ |
| A .....         |          | $19.9 \pm 0.2$ | 1.78                  | 1.6                | 60                 | $-0.70 \pm 0.05$ | 5.9               | $7.5 \pm 1.5$ |
| B1+B2+B3 .....  |          | $21.7 \pm 0.3$ | 5.61                  | 1.3                | (19)               | $(-0.8 \pm 0.1)$ | 6.9               | $(6 \pm 1.5)$ |
| D .....         |          | $22.0 \pm 0.5$ | 2.94                  | 1.6                | (18)               | $(-0.8 \pm 0.1)$ | 1.6               | $(5 \pm 1.5)$ |
| E .....         |          | $22.3 \pm 0.3$ | 3.77                  | 1.4                | (9)                | $(-0.8 \pm 0.1)$ | 2.2               | $(5 \pm 1.5)$ |
| 3C 371          |          |                |                       |                    |                    |                  |                   |               |
| Jet total ..... | <i>V</i> | $20.9 \pm 0.2$ | ...                   | ...                | 181                | $-0.75 \pm 0.06$ | 7.04              | $5.8 \pm 0.9$ |
| A .....         |          | $21.7 \pm 0.3$ | 3.13                  | 1.15               | 93                 | $-0.76 \pm 0.05$ | 2.05              | $6.8 \pm 0.8$ |
| B .....         |          | $23.1 \pm 0.7$ | 1.68                  | 0.7                | ...                | $(-0.76)$        | 0.44              | $6.9 \pm 2.2$ |
| C .....         |          | ...            | 0.46                  | ...                | ...                | ...              | ...               | ...           |
| D .....         |          | $24.3 \pm 0.8$ | 4.52                  | ...                | ...                | ...              | ...               | ...           |
| PKS 2201+044    |          |                |                       |                    |                    |                  |                   |               |
| A .....         | <i>R</i> | $24.2 \pm 0.1$ | 2.12                  | 0.9                | 9                  | $-0.85 \pm 0.05$ | 0.10              | $8 \pm 1$     |

<sup>a</sup> Values depending on estimated radio fluxes are reported in parentheses.

<sup>b</sup> Distance in arcseconds from center,  $1'' = 1.48, 1.37,$  and  $0.74$  kpc for PKS 0521–365, 3C 371, and PKS 2201+044, respectively. Distance for knot B of PKS 0521–365 corresponds to knot B2.

<sup>c</sup> Jet width at zero intensity in arcseconds orthogonal to the jet axis. Due to the noise the zero intensity is  $\sim 1/20$  of the value in the axis.

<sup>d</sup> Radio flux in mJy. For PKS 0521–365 2 cm radio flux from Keel 1986. Fluxes for structures B, D, and E were estimated by us directly from the radio map of Keel 1986 and are uncertain. For 3C 371, 1.6 GHz radio flux from Akujor et al. 1994. For PKS 2201+044, 5 GHz radio flux estimated by us from the radio map of Laurent-Muehleisen et al. 1993.

<sup>e</sup> Volume of the structure in  $\text{kpc}^3$ .

<sup>f</sup> Intensity of the equipartition magnetic field in  $10^{-5}$  G.

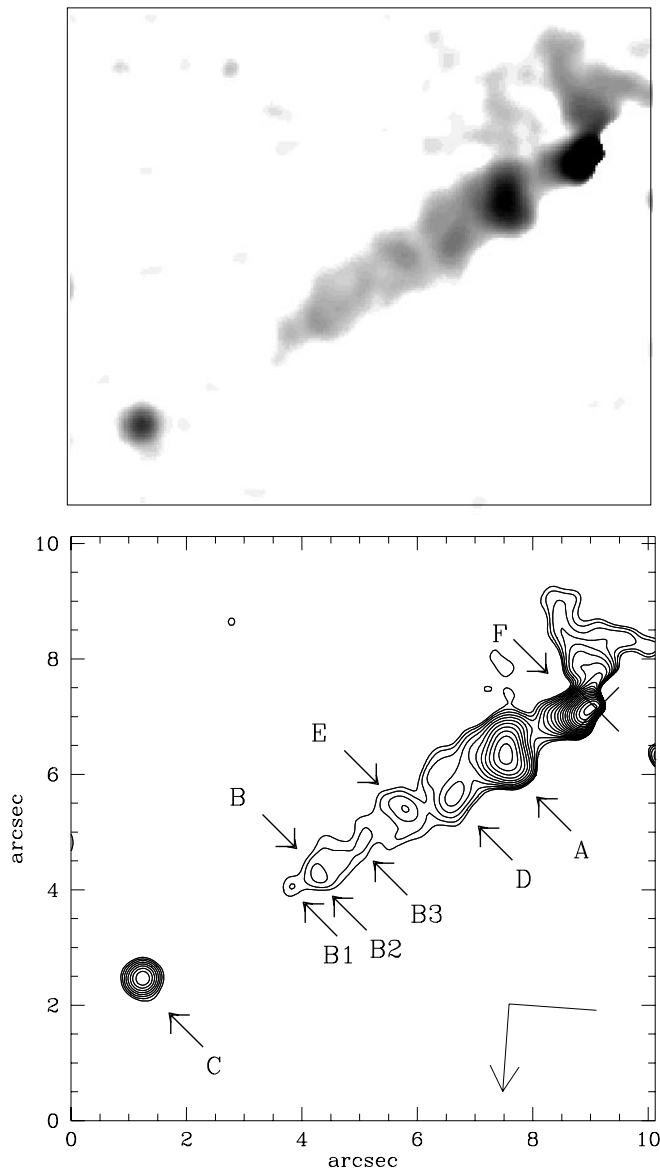


FIG. 1.—Upper panel: F702W image of the optical jet of PKS 0521–365, obtained after subtracting the central point source and a galaxy model. To improve the visibility of jet features, a Gaussian filter with  $\sigma = 3$  pixels was applied, reducing the resolution to  $0''.14$ . Lower panel: Contour plot of the above image, with knots labeled. North and east are as indicated. The big cross at the upper right indicates the position of the central point source. Note that the diffuse emission detected southwest of the point source was never reported before and can actually be due to imperfect subtraction of the host galaxy. Isophotes are 0.25 mag apart, starting from  $\mu_R = 21.9$  mag arcsec $^{-2}$ .

ground-based images, in its terminal region the jet looks much more diffuse than previously reported. At the lowest surface brightness reached in our observations, the jet has an almost constant width (as is also the case in the deeper image obtained by Falomo 1994). Even in knot A, where the jet is very bright, the full width at zero intensity is not significantly larger than in the other zones. Only at the very end, at B1, is the jet narrower. Present data therefore suggest the plasma is moving in a well-defined cylindrical funnel.

The optical morphology of the jet agrees very well with what is observed at 2 cm (Keel 1986). The general shape and the total length of the radio jet are almost exactly repro-

duced in the optical. This is particularly true for knot A, which is well resolved in both bands (Fig. 2).

The 2 cm flux was given by Keel (1986) for the whole jet, knot A, and the jet minus A. For other three knots we estimated 2 cm flux directly from the radio map of Keel (1986). We then evaluated the radio-to-optical spectral index for four knots and the full jet (Table 1). It turns out that  $\alpha_{RO}$  is relatively stable along the jet; indeed, all values are consistent within the errors. This is simply a quantitative confirmation of the general one-to-one morphological correspondence between the two bands.

Assuming equipartition between particles and magnetic field, the internal magnetic field can be estimated knowing the total flux and volume of a radio source. In our case, the size of the emitting knots can be directly measured on the image and transformed into volume assuming symmetry. We report in Table 1 the volume  $V$  of the whole jet and of each knot. The jet is assumed to be a cylinder of diameter  $1''.5$  and length  $5''$ . For the knots we assumed spherical symmetry, reporting in Table 1 the volume of the sphere which has projected surface equal to the knot surface. This was done because the jet is resolved orthogonal to its axis, with the knots occupying only a fraction of the jet width.

The complete radio-to-optical flux energy distribution of the synchrotron emission from the jet alone is not known. We therefore assume the synchrotron emission from jet and knots is described by power laws, with spectral indices as reported in Table 1, extending from  $\nu \sim 10^7$  to  $10^{15}$  Hz. The upper frequency limit is set by the *HST* FOC data at 3200 Å (Macchetto et al. 1991) and has basically no effect on the estimated equipartition magnetic field. With these assumptions, the jet has almost constant  $B_{eq} = 6 \times 10^{-5}$  G along its length (Table 1). Magnetic fields of this intensity are commonly observed in radio sources, and our values are fully consistent with the value of  $B_{eq} = 5 \times 10^{-5}$  G reported by Keel (1986).

### 3.2. 3C 371

This extragalactic radio source has been the subject of intense study at many frequencies. It was first classified as an optically violently variable quasar (Angel & Stockman 1980) and then as a radio-selected BL Lac object (Giommi

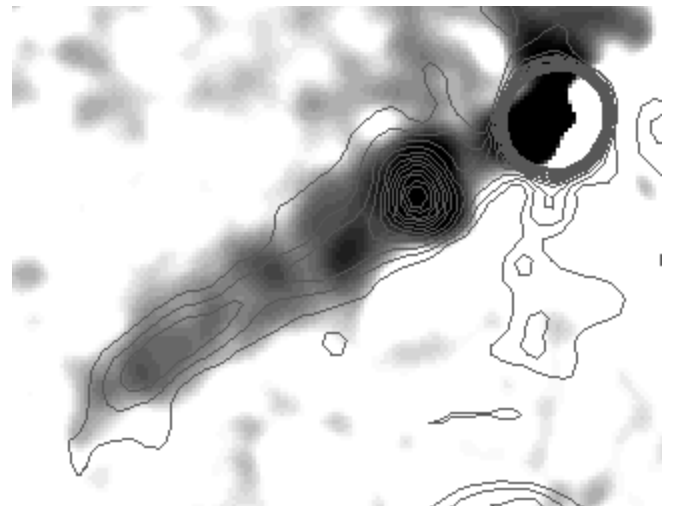


FIG. 2.—Optical image of the PKS 0521–365 jet (gray scale), overlaid with contours of the VLA 2 cm radio map which has resolution of  $0''.3$  (Keel 1986).

et al. 1990). The radio morphology is dominated by a one-sided jet emanating from the central core and extending up to  $25''$  from the nucleus, ending at one of the two radio lobes (Wrobel & Lind 1990). This morphology is characteristic of a Fanaroff-Riley type II radio source. In the optical band 3C 371 is hosted by a large elliptical galaxy (UGC 11130: Condon & Broderick 1988) at  $z = 0.0508$  (Sandage 1973), surrounded by a small cluster of galaxies (Stickel, Fried, & Kühr 1993). Recently the optical counterpart of the radio jet was discovered by Nilsson et al. (1997). As observed from the ground, the optical jet extends only a few arcseconds from the nucleus, ending in a bright knot where the radio jet apparently changes direction.

At *HST* resolution, the jet is fully resolved also perpendicular to the jet axis. At least three bright knots are clearly visible (Fig. 3). Near the center, the jet starts with a bright structure (C), followed by a much smaller knot (B) which is elongated orthogonal to the jet. Farther out is the broadest structure, knot A,  $\sim 1''.3$  wide. In our *HST* image, the optical jet appears to extend beyond A; the narrow structure named D in Figure 3 coincides with a faint feature visible in the Nilsson et al. (1997) image. The beginning of feature D is possibly also visible in the MERLIN map of Akujor et al. (1994).

Comparing optical and radio emission, a general one-to-one matching of all knots is found. The observed radio jet (Wrobel & Lind 1990) is several times longer than the optical jet. Compared to PKS 0521–365 and M87, this is the most obvious difference. It must be noted that the radio flux fades significantly after knot A. Wrobel & Lind (1990) report a peak flux of 3.8 mJy from the final hot spot of the radio jet. Assuming  $\alpha_{\text{RO}} = -0.7$  (Table 1) the expected flux in *V* band is  $\lesssim 5.7 \times 10^{-4}$  mJy, roughly 1 mag fainter than the limit of our observation. Hence, present data are consistent with a constant  $\alpha_{\text{RO}}$  and general correspondence of radio and optical emission, and deeper images may well be able to detect optical emission up to the very end of the radio jet. On the contrary, if the optical jet actually ends at A, it would be even more interesting, offering an important benchmark for theoretical models to explain the propagation of electrons and magnetic field through the interstellar medium. Deeper optical observations are therefore highly desirable.

Under the same set of assumptions adopted for PKS 0521–365 about synchrotron power-law spectrum and emission volume, we estimate the physical properties of the jet. In Table 1 the *V* magnitude and volume for the whole jet and main knots are reported. Knot C is too close to the central point source so we do not attempt to measure its luminosity. To estimate the volume of the jet we modeled it as a cylinder with diameter of 1 and length  $3''.5$ , while spherical symmetry was assumed in computing the volume of knots. The radio flux at 1.6 GHz (Akujor et al. 1994) is also quoted.

The same value of the radio-to-optical spectral index is found both for the whole jet and for knot A. Considering the *H*- and *B*-band data from Nilsson et al. (1997) together with our *V*-band data, the near-IR–optical spectral index of knot A is  $\alpha_{\text{IR-O}} = -0.63 \pm 0.2$ . This is fully consistent with  $\alpha_{\text{RO}}$ , indicating no steepening of the radiation spectrum at high frequencies.

The equipartition magnetic field is basically constant along the jet and has average intensity  $B_{\text{eq}} = 6.5 \times 10^{-5}$  G, similar to what was found for PKS 0521–365.

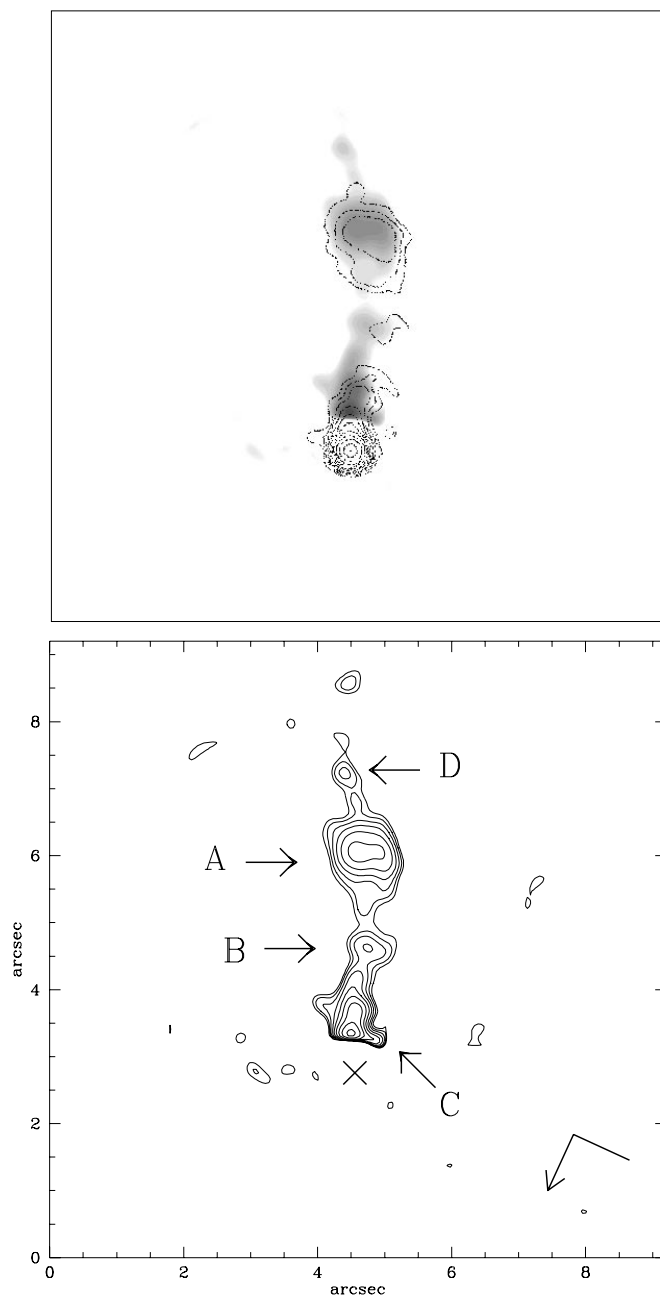


FIG. 3.—Upper panel: The F555W gray-scale image of the optical jet of 3C 371, obtained after subtracting the central point source and a galaxy model, smoothed with a Gaussian filter with  $\sigma = 3$  pixels, reducing the resolution down to  $0''.14$ . Overplotted on the optical image is a contour plot of the 1.6 GHz radio map by Akujor et al. (1994). Lower panel: Contour plot of the above optical image. North and east are as indicated. The big cross indicates the position of the central point source. Isophotes are 0.25 mag apart, starting from  $\mu_V = 23.3$  mag arcsec $^{-2}$ .

### 3.3. PKS 2201+044

This source is a nearby ( $z = 0.028$ ) BL Lac object (Angel & Stockman 1980) hosted in a prominent elliptical galaxy (Falomo 1996; Scarpa et al. 1999). The optical spectrum shows emission and absorption lines and is similar to Seyfert 1 spectra (Veron-Cetty & Veron 1993; Falomo, Scarpa, & Bersanelli 1994). The associated radio source has a total extent of  $5''.6$  (Ulvestad & Johnson 1984) and is core dominated (Preston et al. 1985). The radio properties of PKS 2201+044 have been thoroughly investigated by

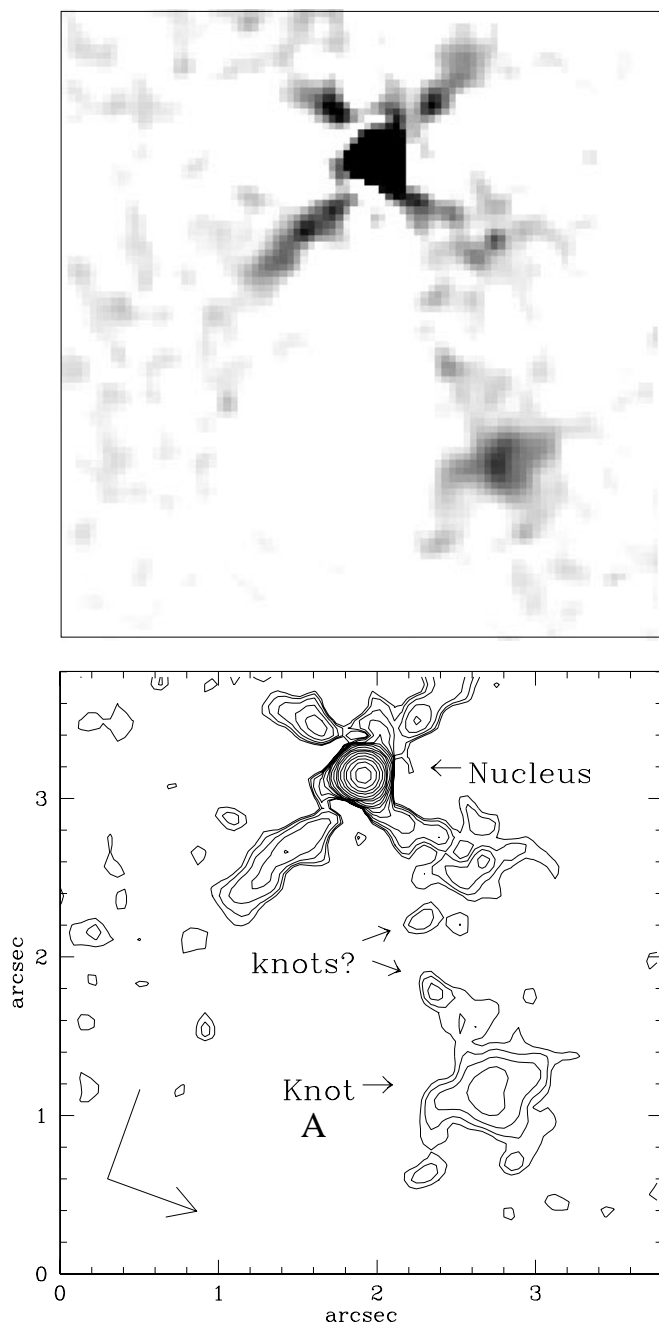


FIG. 4.—Upper panel: F702W image of the optical jet of PKS 2201+044. In this source the central point source is not very bright, so here we show the image after subtraction of the galaxy only. The point source (nucleus) is characterized by the four diffraction spikes, not to be confused with the jet. To improve the visibility of faint structures, a Gaussian filter with  $\sigma = 1$  pixel was applied. Lower panel: Contour plot of the above image. North and east are as indicated. Knot A is  $2''.12$  from the nucleus. Two more knots most probably associated with the jet are also marked. Isophotes are  $0.5$  mag apart, starting from  $\mu_R = 23.2$  mag arcsec $^{-2}$ .

Laurent-Muehleisen et al. (1993), who found a core-jet morphology, with the jet extending for more than 10 kpc. A bright radio hot spot was also found 1.5 kpc ( $2''$ ) from the nucleus.

At *HST* resolution the optical source is fully resolved into nucleus, host galaxy, and jet. Thanks to the superior spatial resolution, some structures of the jet are directly visible above the strong background of the host galaxy. In Figure 4 we show the residuals after subtraction of the best-

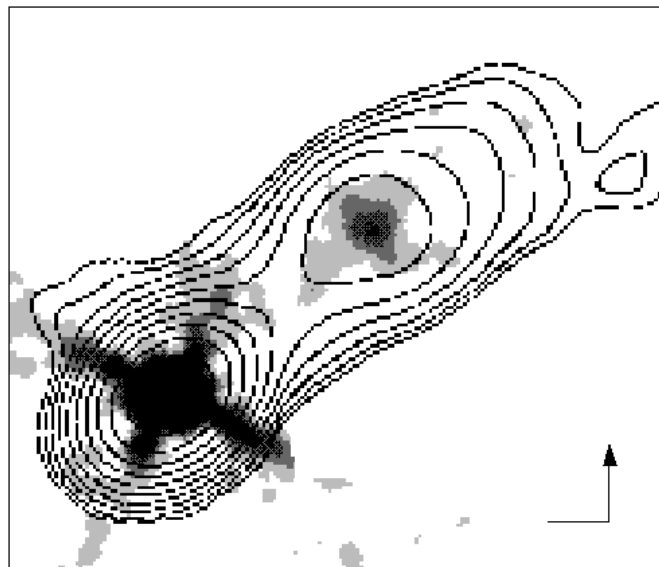


FIG. 5.—The WFPC2 F702W gray-scale image of the jet of PKS 2201+044, overlaid with contours of the 5 GHz radio map from Laurent-Muehleisen et al. (1993), which has lower resolution than the *HST* data. The *HST* image has been rotated so that north is up and east is on the left.

fit galaxy model. The jet structure appears at position angle  $310^\circ$ , with the most prominent knot  $2''.12$  (1.57 kpc) from the nucleus. Comparing our data to the 5 GHz radio map of Laurent-Muehleisen et al. (1993), a clear correspondence of this bright optical knot with the brightest radio knot is found, strongly supporting the association of the optical structure with the synchrotron radio jet (Fig. 5). Unfortunately, the resolution of the radio map is insufficient to resolve further structures.

The brightest optical knot is clearly resolved both along and perpendicular to the jet axis and has quite a complicated structure, extending over a region of  $\sim 0''.5 \times 0''.9$ . Between the knot and the nucleus some weaker knots may also be present.

The integrated magnitude of knot A is  $m_R = 24.2 \pm 0.1$  mag ( $5.7 \times 10^{-4}$  mJy). Its radio flux is  $\sim 9$  mJy at 5 GHz, corresponding to radio-to-optical spectral index  $\alpha_{RO} = -0.85$ , fully consistent with the values found in others optical jets (Crane et al. 1993; Scarpa & Urry 1999).

Assuming the knot is a sphere of radius  $0''.4$ , and adopting the same set of hypotheses as for the previous two jets, the equipartition magnetic field is  $B_{eq} = 8 \times 10^{-5}$  G, again similar to what is found in other jets.

#### 4. CONCLUSIONS

We have described *HST* observations of three synchrotron jets detected at optical wavelengths in three BL Lac objects. In two cases, PKS 0521–365 and 3C 371, the jet is fully resolved and several knots can be studied separately. In spite of the clumpiness of the emission, both jets are rather homogeneous, with basically constant values of  $\alpha_{RO} \sim -0.7$  and equipartition magnetic field along the length of the jet. For knot A in 3C 371, a similar spectral index is also found at near-IR–optical frequencies, indicating no significant aging of the radiating electrons.

We also reported the discovery of an optical counterpart of the radio jet of PKS 2201+044. The brightest knot, at

projected distance 1.57 kpc from the nucleus, is fully resolved in the optical. It corresponds precisely to the brightest radio knot, confirming its association with the synchrotron jet. Estimates of  $\alpha_{\text{RO}} = -0.85$  and equipartition magnetic field  $B_{\text{eq}} = 8 \times 10^{-5}$  G are similar to values generally found in other jets. However, to fully understand the morphology of this jet, deeper optical images and higher resolution radio maps are needed.

We note that all three sources exhibit strong emission lines in their optical spectrum, and in PKS 2201+044 and PKS 0521–365 broad emission lines are also observed (Ulrich 1981; Veron-Cetty, & Veron 1993; Scarpa, Falomo, & Pian 1995). This may suggest that in these objects the beaming is modest, and in fact there are indications of this in the case of PKS 0521–365 (Pian et al. 1996). A modest beaming may be consistent with an easier observability of the optical jet. However, our sample is obviously too restricted to elaborate further.

At present, including the newly discovered jet in PKS 2201+044, a total of 14 optical jets are known. This number is not big, but it starts to be large enough to enable decent statistical consideration. It is well known that in all these jets the inferred electron lifetimes are much smaller than needed to explain the jet length, so that reacceleration along the jet seems unavoidable. This is also true for the jet in PKS 2201+044. However, the observed constancy of  $\alpha_{\text{RO}}$  is difficult to explain if electrons are reaccelerated by first-order Fermi mechanism at strong shocks (Heinz & Begelman 1997, and references therein), so that present observations add difficulties to the already hard problem of finding a plausible physical mechanism for electron reacceleration. The possibility of electrons being transported in a

loss-free channel inside the jet (Owen, Hardee, & Cornwell 1989) is difficult to accept, because *HST* observations of M87 have shown the optical emission is centered near the axis of the jet rather than on the edge (Sparks, Biretta, & Macchetto 1996), which appear to be the case also for PKS 0521–365. It is possible that the presence of relativistic motion on kiloparsec scales is common, as supported by direct observations with *HST* of superluminal proper motion in M87 (Biretta et al. 1999). If this is generally the case, then relativistic beaming of the emission is unavoidable, implying that both the intrinsic luminosity of the jet and the equipartition magnetic field are smaller than what we estimated, while electron lifetimes are longer and the necessity for reacceleration is weakened.

An alternative hypothesis is to renounce the basic assumption of equipartition of energy between relativistic particles and magnetic field; the electron lifetimes are longer by approximately the factor  $(B_{\text{eq}}/B)^{1.5}$ . Using a statistical approach we address general considerations of jets' power, beaming, and physical conditions in a companion paper (Scarpa & Urry 1999).

It is a pleasure to thank G. Ghisellini and F. Macchetto for helpful and encouraging comments. We also thank the referee W. C. Keel for helpful comments and for providing the radio map of PKS 0521–365 in fits format. Support for this work was provided by NASA through grant GO-06363.01-95A from the Space Telescope Science Institute, which is operated by AURA, Inc., under NASA contract NAS 5-26555, and by the Italian Ministry for University and Research (MURST) under grant Cofin98-02-32.

#### REFERENCES

- Akujor, C. E., Lüdke, E., Browne, I. W. A., Leahy, J. P., Garrington, S. T., Jackson, N., & Thomasson, P. 1994, *A&AS*, 105, 247  
 Angel, J. R. P., & Stockman, H. S. 1980, *ARA&A*, 18, 321  
 Biretta, J. A., Perlman, E., Sparks, W. B., & Macchetto F. 1999, *BAAS*, 193, 07.09  
 Condon, J. J., & Broderick, J. J. 1988, *AJ*, 96, 30  
 Crane, P., et al. 1993, *ApJ*, 402, L37  
 Danziger, I. J., Fosbury, R. A. E., Goss, W. M., & Ekers, R. D. 1979, *MNRAS*, 188, 415  
 Falomo, R. 1994, *Messenger*, 77, 49  
 ———. 1996, *MNRAS*, 283, 241  
 Falomo, R., Scarpa, R., & Bersanelli, M. 1994, *ApJS*, 93, 125  
 Falomo, R., Urry, C. M., Scarpa, R., Pesce, J.E., Giavalisco, M., & Treves, A. 1999, in preparation  
 Giommi, P., Barr, P., Pollock, A. M. T., Garilli, B., & Maccagni, D. 1990, *ApJ*, 356, 432  
 Heinz, S., & Begelman, M. C. 1997, *ApJ*, 490, 653  
 Holtzman, J. A., Burrows, C. J., Casertano, S., Hester, J. J., Trauger, J. T., Watson, A. L., & Worthey, G. 1995, *PASP*, 107, 1065  
 Keel, W. C. 1986, *ApJ*, 302, 296  
 Krist, J. 1995, in *Astronomical Data Analysis, Software and Systems IV*, ed. R. Shaw et al. (San Francisco: ASP), 349  
 Laurent-Muehleisen, S. A., Kollgaard, R. I., Moellenbrock, G. A., & Feigelson, E. D. 1993, *AJ*, 106, 875  
 Macchetto, F., Albrecht, R., Barbieri, C., et al. 1991, *ApJ*, 369, L55  
 Nilsson, K., Heidt, J., Pursimo, T., Sillanpää, A., Takalo, L. O., & Jäger, K. 1997, *ApJ*, 484, L107  
 O'Dea, C. P., De Vries, W., Biretta, J. A., & Baum, S. A. 1999, *AJ*, 117, 1143  
 Owen, F. N., Hardee, P. E., & Cornwell, T. J. 1989, *ApJ*, 340, 698  
 Pian, E., Falomo, R., Ghisellini, G., Maraschi, L., Sambruna, R. M., Scarpa, R., & Treves, A. 1996, *ApJ*, 459, 169  
 Preston, R. A., Morabito, D. D., Williams, J. G., Faulkner, J., Jauncey, D. L., & Nicolson, G. D. 1985, *AJ*, 90, 1599  
 Ridgway, S. E., & Stockton, A. 1997, *AJ*, 114, 511  
 Sandage, A. 1973, *ApJ*, 180, 687  
 Scarpa, R., Falomo, R., & Pian, E. 1995, *A&A*, 303, 730  
 Scarpa, R., & Urry, C. M. 1999, in preparation  
 Scarpa, R., Urry, C. M., Falomo, R., Pesce, J. E., & Treves, A. 1999, *ApJ*, submitted  
 Sparks, W. B., Biretta, J. A., & Macchetto, F. 1994, *ApJS*, 90, 909  
 ———. 1996, *ApJ*, 473, 254  
 Sparks, W. B., et al. 1995, *ApJ*, 450, L55  
 Sparks, W. B., Miley, G. K., & Macchetto, F. 1990, *ApJ*, 361, L41  
 Stickel, M., Fried, J. W., & Kühr, H. 1993, *A&AS*, 98, 393  
 Ulrich, M. E. 1981, *A&A*, 103, L1  
 Ulvestad, J. S., & Johnston, K. J. 1984, *AJ*, 89, 189  
 Urry, C. M., Scarpa, R., O'Dowd, M., Falomo, R., Pesce, J. E., & Treves, A. 1999, *ApJ*, submitted  
 Veron-Cetty, M. P., & Veron, P. 1993, *A&AS*, 100, 521  
 Wrobel, J. M., & Lind, K. R. 1990, *ApJ*, 348, 135